Polyhedron 58 (2013) 190–196

Contents lists available at SciVerse ScienceDirect

Polyhedron

journal homepage: www.elsevier.com/locate/poly

New heme–dioxygen and carbon monoxide adducts using pyridyl or imidazolyl tailed porphyrins

Yuqi Li, Savita K. Sharma, Kenneth D. Karlin *

Department of Chemistry, The Johns Hopkins University, Baltimore, MD 21218, United States

ARTICLE INFO

Article history:
Available online 20 November 2012

Keywords:
Base tethered heme complexes
Reduced heme–Fe^{II} complexes
Heme–Fe^{III}–superoxo complexes
Heme–Fe^{II}–carbonyl complexes
^{1,2}H NMR spectroscopy

ABSTRACT

Inspired by the chemistry relevant to dioxygen storage, transport and activation by metalloproteins, in particular for heme/copper oxidases, and carbon monoxide binding to metal-containing active sites as a probe or surrogate for dioxygen binding, a series of heme derived dioxygen and CO complexes have been designed, synthesized, and characterized with respect to their physical properties and reactivity. The focus of this study is in the description and comparison of three types heme–superoxo and heme–CO adducts. The starting point is in the characterization of the reduced heme complexes, $[(F_8)Fe^{II}]$, $[(P^{Py})Fe^{II}]$ and $[(P^{Im})Fe^{II}]$, where F_8, P^{Py} and P^{Im} are iron(II)–porphyrinates and where P^{Py} and P^{Im} possess a covalently tethered axial base pyridyl or imidazolyl group, respectively. The spin-state properties of these complexes vary with solvent. The low temperature reactions between O_2 and these reduced porphyrin Fe^{II} complexes yield distinctive low spin heme–superoxo adducts. The dioxygen binding properties for all three complexes are shown to be reversible, via alternate argon or O_2 bubbling. Carbon monoxide binds to the reduced heme–Fe^{II} precursors to form low spin heme–CO adducts. The implications for future investigations of these heme O_2 and CO adducts are discussed.

1. Introduction

Heme–O_2 chemistry has a long history, due to its direct relationship to hemoglobin and myoglobin O_2-carrier proteins, and other (per)oxidases (e.g., catalase, chloroperoxidase) or oxygenases (e.g., cytochrome P-450 monooxygenase) [1,2]. Our own interest is in relationship to heme/copper oxidases such as cytochrome *c* oxidase (CcO). CcO is responsible for O_2-reduction to water as a terminal step of respiratory chain of mitochondria and many aerobic bacteria [3–7]. The most well established enzyme dioxygen intermediate is proposed to be ferric-superoxo species which is generated upon initial O_2-reaction with the fully reduced heme–iron...Cu center [8]. This forms prior to O–O bond cleavage and has deservedly attracted considerable interest [9–14]. In our synthetic research program inspired by cytochrome c oxidase heme–copper chemistry [15–19], one approach we take is to add copper complexes to pre-formed heme-superoxo species [16–18,20]; thus it is in our strong interest to also fully understand the nature of these iron(II)–dioxygen adducts, the ferric-superoxo species [13,14]. Carbon monoxide has been widely used on metalloproteins as a surrogate for O_2-binding to the active site [21–25] and indeed there exist biological heme CO-sensors [26,27]. CO favors strongly binding to five-coordinated ferrous species to form stable six-coordinate heme–Fe^{II} carbonyl complexes. Determination of either ν(C–O) or Fe–(CO) stretching vibrations can provide insights into the heme–iron environment electronic structure [23,24,28,29]. Laser photoejection of CO and the study of the kinetics of CO-rebinding or "flash and trap" experiments to probe the fast reactions between O_2 and heme Fe^{II} complexes also provides a great deal of fundamental information about the active-site nature and/or the O_2-binding process [25,30–33]. We have even used heme–carbonyl complexes and photoejection of CO, to study transfer of carbon monoxide to copper(I) complexes whereupon the CO ligand returns to iron [33–36]; this process has relevance to CcO (bio)chemistry [22]. Given this history of chemically or biochemically derived heme–CO complexes, further insights into synthetic aspects and physical properties of heme–CO adducts are still needed, and as mentioned, this information is of value for the study of heme–Cu complex chemistry. In this paper we report new iron(II) and iron(III) complexes of an imidazolyl tailed tetraarylporphyrin P^{Im} and a new ligand and iron complexes with a pyridyl tailed porphyrin P^{Py}. Reduced species $(P^{Im})Fe^{II}$ and $(P^{Py})Fe^{II}$ have been synthesized and characterized. Then, we describe O_2 and CO reactivity towards these species, along with $[(F_8)Fe^{II}]$, where F_8 is the same porphyrinate used in P^{Im} and P^{Py}, however lacking a covalently tethered axial base ligand for iron. The CO and O_2 binding to $[(F_8)Fe^{II}]$ will be compared and contrasted with that observed for $[(P^{Py})Fe^{II}]$ and $[(P^{Im})Fe^{II}]$ (Fig. 1).

* Corresponding author.
E-mail address: karlin@jhu.edu (K.D. Karlin).

0277-5387/$ - see front matter © 2012 Elsevier Ltd. All rights reserved.
http://dx.doi.org/10.1016/j.poly.2012.11.011

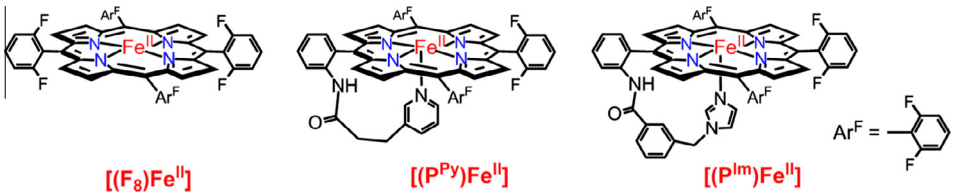

Fig. 1. Porphyrinate–Fe^{II} complexes used in the present study.

2. Results and discussion

2.1. Heme–Fe^{II} complexes and solvent dependent spin-states

The reduced Fe^{II} hemes employed are: (i) [$(F_8)Fe^{II}$] (F_8 = tetrakis(2,6 difluorophenyl)porphyrinate), which was previously described [14,18,19], (ii) a recently reported porphyrinate P^{Im} [37], which until now has only been used for heme nitric oxide chemistry; here we develop the reduced heme [$(P^{Im})Fe^{II}$] and small molecule (O_2, CO) binding chemistry, and (iii) [$(P^{Py})Fe^{II}$], a completely new porphyrinate which employs a tailed pyridyl moiety as axial base. Workable quantities of heme complexes [$(F_8)Fe^{II}$], [$(P^{Py})Fe^{II}$] and [$(P^{Im})Fe^{II}$] have been prepared and characterized by ESI-MS, UV–Vis and ^{1,2}H NMR spectroscopies (see Section 4).

We previously reported that the spin state of [$(F_8)Fe^{II}$] is dependent on the solvent used [14]. Based on ^{2}H NMR spectra, where pyrrole-H positions have been replaced by deuterium [14,38–42], [$(F_8)Fe^{II}$] exhibits downfield resonances in acetone as solvent (Table 1), revealing a high-spin Fe^{II} (d^6, $S = 2$) complex state; this indicates pentacoordination with one axially ligated acetone molecule. In tetrahydrofuran (THF), downfield resonances are also observed, thus the complex is five- or six-coordinate with one or two axial THF molecules; a crystal structure of [$(F_8)Fe^{II}(THF)_2$] has been determined [43]). However, we find that acetonitrile (but only at low temperature, i.e., 233 K) and pyridine at all temperatures act as 'strong' ligands. Pyrrole ^{2}H resonances are found in diamagnetic region at δ 10.1 ppm for MeCN (233 K) and δ 8.9 ppm for pyridine as solvent (293 K), indicating a low-spin, six-coordinate ferrous center (d^6, $S = 0$) is present and thus two axial solvent derived molecules ligate.

We further investigated the related properties for the new complexes [$(P^{Py})Fe^{II}$] and [$(P^{Im})Fe^{II}$] using ^{1,2}H NMR spectroscopies. Table 1 provides the chemical shifts for the pyrrole-H resonances for [$(F_8)Fe^{II}$], [$(P^{Py})Fe^{II}$] and [$(P^{Im})Fe^{II}$] in acetone and THF at 293 K. In acetone and THF, the pyrrole-H resonance for [$(P^{Py})Fe^{II}$] are paramagnetically shifted to δ 46, 48 ppm in acetone (Fig. S1a) while in THF they are found at δ 50 and 58 ppm (Fig. S1b). These values are similar to the pyrrole hydrogen shifts observed in [$(F_8)Fe^{II}$], suggesting [$(P^{Py})Fe^{II}$] is a high-spin ferrous complex (d^6, $S = 2$), a five-coordinate species with an axial pyridyl donor derived from the porphyrinate ligand P^{Py}. As is well known for such species, the iron would be expected to be well out of the plane of the prophyrinate toward the side with the pyridyl group to which it coordinates. For [$(P^{Im})Fe^{II}$], in acetone, the pyrrole hydrogens were found at δ 41 and 60 ppm (Fig. S2a) also indicating a high-spin ferrous complex (d^6, $S = 2$), thus as a five coordinate species with an axial ligand tailed imidazole. However in THF, a diamagnetic ^{1}H NMR spectrum was observed and the ^{2}H NMR of the pyrrole-deuterated analog [$(P^{Im}$-$d_8)Fe^{II}$] (which allows direct visualization of only the pyrrole resonances in the diamagnetic region, unobstructed by other proton resonance of the entire porphyrinate, see Fig. S2b) shows that these hydrogens are shifted upfield relative to the $S = 2$ complexes described above, to δ 8.4, 10.9 and 12.6 ppm (Fig. S2b). This indicates that in THF as solvent, [$(P^{Im})Fe^{II}$] is a low-spin ferrous complex (d^6, $S = 0$), possessing two axial ligands, one the imidazole donor which is part of P^{Im} and on the other side of the heme plane, a strongly bound THF molecule.

Table 1
Chemical shifts of the pyrrole-H of [$(F_8)Fe^{II}$], [$(P^{Py})Fe^{II}$] and [$(P^{Im})Fe^{II}$] at various temperatures in various solvents.

	Solvent		
	THF	Acetone	Ref.
$\delta_{pyrrole}$ ([$(F_8)Fe^{II}$], 293 K) (ppm)	56	48	[14]
$\delta_{pyrrole}$ ([$(P^{Py})Fe^{II}$], 293 K) (ppm)	50, 58	46, 48	This work
$\delta_{pyrrole}$ ([$(P^{Py})Fe^{II}$], 193 K) (ppm)	99, 88	86, 92	This work
$\delta_{pyrrole}$ ([$(P^{Im})Fe^{II}$], 293 K) (ppm)	8.4, 10.9, 12.6	41, 60	This work
$\delta_{pyrrole}$ ([$(P^{Im})Fe^{II}$], 193 K) (ppm)	9.5		This work

2.2. Reversible heme–Fe–superoxo formation

We previously reported on the complex [$(THF)(F_8)Fe^{III}(O_2^{\cdot-})$], λ_{max} = 416, 536 nm (in tetrahydrofuran solvent), as a six coordinate low-spin ferric superoxo complex that shows a diamagnetic NMR spectrum; the pyrrole hydrogens or deuterium were found at δ 8.9 ppm. It was generated by reversible binding of O_2 to [$(F_8)Fe^{II}$] at low temperature (193 K) and where bubbling the solution with argon gas reversed the binding, regenerating [$(F_8)Fe^{II}$] (Scheme 1) [14]. Titrations indicating 1:1 uptake of O_2 for each [$(F_8)Fe^{II}$] precursor also strongly supports the [$(THF)(F_8)Fe^{III}(O_2^{\cdot-})$] formulation. Confirmation that this complex is best described as an iron(III)-

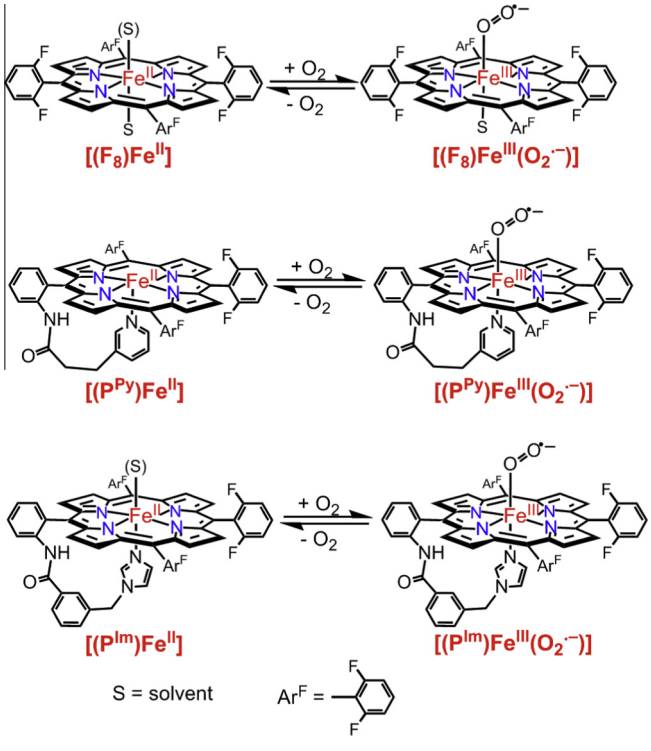

Scheme 1.

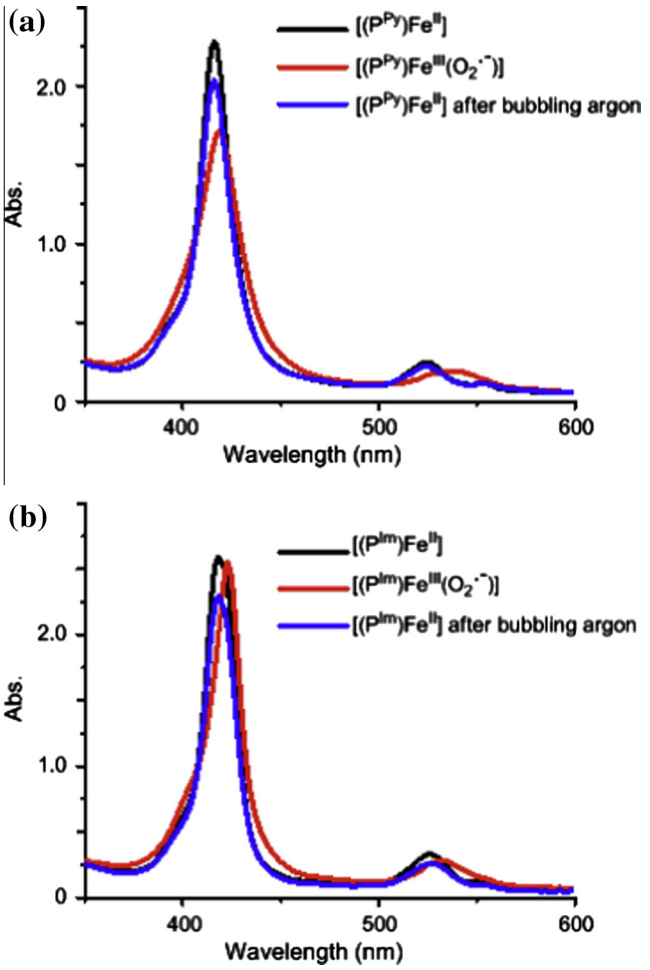

Fig. 2. (a) UV–Visible spectra of the heme iron (III)–superoxo complex [$(P^{Py})Fe^{III}(O_2^{\cdot-})$] (red, λ_{max} = 419, 535 nm) formed after bubbling O_2 into a solution of [$(P^{Py})Fe^{II}$] (black, λ_{max} = 417, 524, 553 nm) at 193 K in THF. Subsequent bubbling of argon through the [$(P^{Py})Fe^{III}(O_2^{\cdot-})$] solution reverses the O_2 binding to give back [$(P^{Py})Fe^{II}$] (blue, λ_{max} = 417, 524, 553 nm). (b) UV–Visible spectra of the heme iron(III)–superoxo complex [$(P^{Im})Fe^{III}(O_2^{\cdot-})$] (red, λ_{max} = 423, 534 nm) after bubbling O_2 into solution of [$(P^{Im})Fe^{II}$] (black, λ_{max} = 417, 525, 553 nm) at 193 K in THF. Argon bubbling through the [$(P^{Im})Fe^{III}(O_2^{\cdot-})$] solution reversed O_2 binding to give back [$(P^{Im})Fe^{II}$] (blue, λ_{max} = 417, 525, 553 nm). (Colour online.)

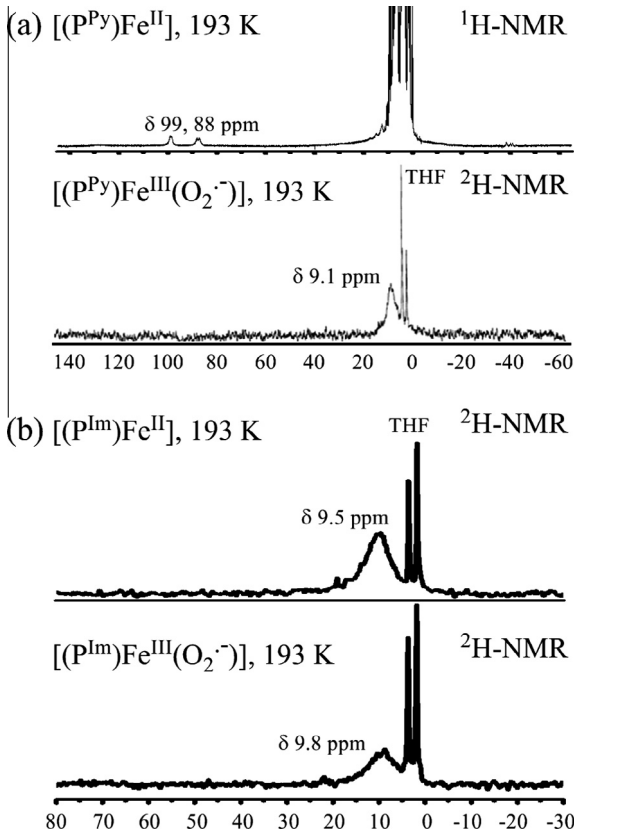

Fig. 3. (a) ^{1}H NMR spectrum [$(P^{Py})Fe^{II}$] ($\delta_{pyrrole}$ = 88, 99 ppm) and ^{2}H NMR spectrum of [$(P^{Py})Fe^{III}(O_2^{\cdot-})$] ($\delta_{pyrrole}$ = 9.1 ppm) at 193 K in THF. (b) ^{2}H NMR spectrum of [$(P^{Im})Fe^{II}$] ($\delta_{pyrrole}$ = 9.5 ppm) and [$(P^{Im})Fe^{III}(O_2^{\cdot-})$] ($\delta_{pyrrole}$ = 9.8 ppm) at 193 K in THF.

superoxide species, in terms of its electronic structure, come from resonance Raman spectroscopy: $\nu_{(O-O)}$ = 1178 cm^{-1} [$\Delta(^{18}O_2)$ −64 cm^{-1}], $\nu_{(Fe-O)}$ = 569 cm^{-1} [$\Delta(^{18}O_2)$ −24 cm^{-1}] [44,45].

Here, we show that new heme–superoxo complexes form using the porphyrinates with a tailed pyridyl (P^{Py}) or imidazolyl (P^{Im}) as an axial ligand. Upon O_2 addition via bubbling to a 193 K THF solution of [$(P^{Py})Fe^{II}$], with λ_{max} (ε/mM^{-1} cm^{-1}): 417 (210.5), 524 (22.0), 553 nm (8.7), there is an immediate change to give a new species which is stable at this temperature, the heme–superoxo complex formulated as [$(P^{Py})Fe^{III}(O_2^{\cdot-})$] (Scheme 1), with λ_{max} (ε/mM^{-1} cm^{-1}): 419 (157.0), 535 (17.6) (Fig. 2a). Upon bubbling argon through this solution, UV–Vis monitoring suggests that O_2-binding is slowly reversed giving back [$(P^{Py})Fe^{II}$] (Fig. 2a). The reversible O_2-binding was also observed when the chemistry was carried out in the non-coordinating solvent CH_2Cl_2, but the reversal occurs much more slowly; Ar bubbling and warming the solution to RT is required to remove all of the O_2 (Fig. S3a). Similar chemistry occurred when employing [$(P^{Im})Fe^{II}$] as the starting complex. When O_2 is added to the solution of [$(P^{Im})Fe^{II}$] in THF at 193 K [λ_{max} (ε/mM^{-1} cm^{-1}): 417 (258.6), 525 (28.6), 553 nm (7.2)], a complex formulated as [$(P^{Im})Fe^{III}(O_2^{\cdot-})$] is reversibly formed [$\lambda_{max}$ (ε/mM^{-1} cm^{-1}): 423 (247.4), 534 (23.0)] (Fig. 2b). The reversible O_2-binding to [$(P^{Im})Fe^{II}$] in CH_2Cl_2 also required bubbling argon through the [$(P^{Im})Fe^{III}(O_2^{\cdot-})$] containing solution while warming to room temperature (Fig. S3b).[1]

NMR spectroscopic studies were also performed on these base tailed heme–superoxo complexes [$(P^{Py})Fe^{III}(O_2^{\cdot-})$] and [$(P^{Im})Fe^{III}(O_2^{\cdot-})$]. By directly bubbling O_2 through a THF solution of [$(P^{Py})Fe^{II}$] (δ 99, 88 ppm, high-spin d^6) in a septa closed NMR tube, ^{1}H NMR experiments at 193 K revealed formation of a diamagnetic spectrum, with pyrrole hydrogen shifts occurring at δ 9.1 ppm (Fig. 3a). Confirmation of the assignment came from ^{2}H NMR spectroscopy employing a pyrrole-deuterated analog [$(P^{Py}$-$d_8)Fe^{II}$] as the starting complex. All of this data is consistent with the formulation of a low-spin Fe^{III} (d^5), six coordinate heme–superoxo complex formulated as [$(P^{Py})Fe^{III}(O_2^{\cdot-})$]. As is known from classical studies on hemoglobin and model compounds [9,21], the unpaired electron of the low-spin Fe^{III} ion is antiferromagnetically coupled with the unpaired electron of the superoxide radical anion $O_2^{\cdot-}$, making the complex diamagnetic. Upon bubbling O_2 through a solution of pyrrole-deuterated analog [$(P^{Im}$-$d_8)Fe^{II}$] in THF (δ 9.5 ppm, low-spin d^6), ^{2}H NMR spectroscopy indicates the pyrrole hydrogens resonate at δ 9.8 ppm (Fig. 3b), again suggesting a low-spin Fe^{III} (d^5), six-coordinate heme–superoxo complex formulated as [$(P^{Im})Fe^{III}(O_2^{\cdot-})$]. These features are similar to previously described complex [$(THF)(F_8)Fe^{III}(O_2^{\cdot-})$], where we excluded the possibility of formation of other possible heme–Fe/O_2 adducts, such as

[1] *Note:* the shift of the Soret band for heme–superoxo complexes, as compared to their Fe(II) precursors, can be to lower or higher energies (or even unchanged), depending on the particular ligand system, or the solvent [58,59].

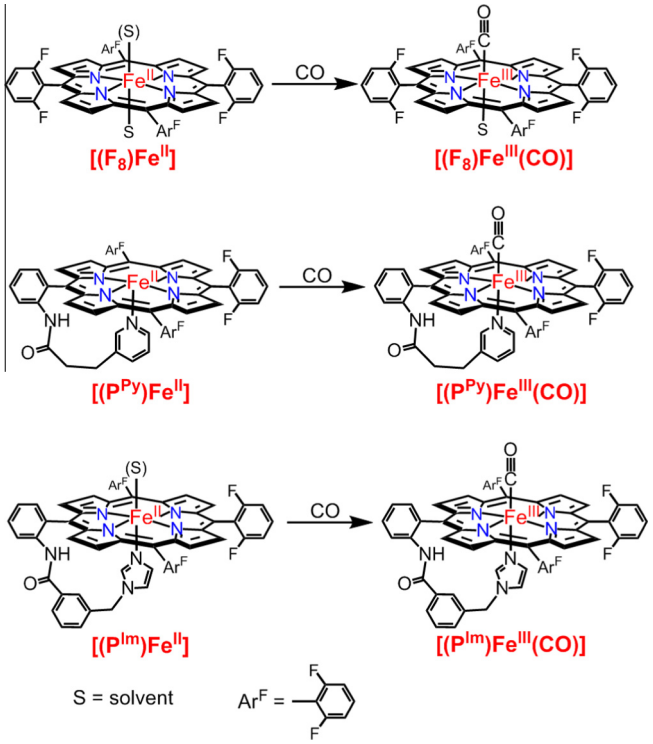

Scheme 2.

Table 2
Comparison of C–O stretching frequencies for carbonyl adducts of $[(F_8)Fe^{II}]$, $[(P^{Py})Fe^{II}]$ and $[(P^{Im})Fe^{II}]$ in various solvents at 293 K.

	Solvent			
	THF	Acetone	CH_2Cl_2	Ref.
ν_{C-O} ($[(F_8)Fe^{II}(C-O)]$) (cm^{-1})	1980	1973	1979, 2040	This work
ν_{C-O} ($[(P^{Py})Fe^{II}(C-O)]$) (cm^{-1})	1985	1980	1985	This work
ν_{C-O} ($[(P^{Im})Fe^{II}(C-O)]$) (cm^{-1})	1985	1980	1985	This work

a binuclear peroxo bridged diiron(III) compound Fe–O–O–Fe, based on the pyrrole hydrogen resonance assignments [14,46,47].

Given the close similarity of certain of the features for the three $Fe^{III}(O_2^{\cdot-})$ complexes reported here, the porphyrinate which they share in common, their NMR spectroscopic properties, and the resonance Raman features previously described for $[(THF)(F_8)Fe^{III}(O_2^{\cdot-})]$ (see above), we can conclude that they are all low-spin six-coordinate with end-on (and not side-on) binding of the superoxo moiety. The O–O and Fe–O stretching frequencies observed for $[(THF)(F_8)Fe^{III}(O_2^{\cdot-})]$ are consistent with other known six-coordinate end-on bound species, model complexes and hemoglobin [48–50]. Further, these parameters do not match those known for a side-on bound example, $(TPP)Fe(O_2)$ (TPP = tetraphenylporphyrinate) whose infra-red spectroscopic properties were studied in an Ar matrix at 15 K [51].[2]

2.3. Stable heme–Fe carbonyl formation

Carbon monoxide (CO) reacts immediately with the reduced synthetic heme complexes, $[(P^{Py})Fe^{II}]$ and $[(P^{Im})Fe^{II}]$ to yield six-coordinate low-spin heme–Fe carbonyl species similar to that reported for $[(F_8)Fe^{II}]$, namely $[(F_8)Fe^{II}(CO)]$ [43] (Scheme 2). These species were detected by UV–Vis spectroscopy (Fig. S4a and b) and confirmed by infrared (IR) (Fig. S5a–c) and ^1H NMR spectroscopic studies (Fig. S6a and b) (see Supporting Information). Table 2 provides the C–O stretching frequencies for $[(F_8)Fe^{II}(CO)]$, $[(P^{Py})Fe^{II}(CO)]$ and $[(P^{Im})Fe^{II}(CO)]$ in various solvents at 293 K. After bubbling CO into the solution of $[(P^{Py})Fe^{II}]$ in THF at 293 K, the UV–Vis absorption band of $[(P^{Py})Fe^{II}]$ shifts to λ_{max} (ε/mM^{-1} cm^{-1}): 420 (175.1), 538 (17.6) (Fig. S4a) while solution cell IR spectroscopy in various solvents leads to the detection of a single CO stretch at $\nu_{(C-O)}$ = 1985 cm^{-1} in THF (Fig. S5b), a typical value for reduced heme–Fe–CO complexes [43]. The diamagnetic ^1H NMR spectrum observed for $[(P^{Py})Fe^{II}(CO)]$ shows the pyrrole hydrogens to be observed at δ 8.8 ppm (Fig. S6a) indicative of a six coordinate low-spin Fe^{II} ($S = 0$, d^6). The three peaks at δ 4 ~6 ppm are assigned as axial pyridine hydrogens which are shifted upfield relative to their free ligand (i.e., P^{Py}) values, confirming the pyridyl group is bound to the iron atom. $[(P^{Im})Fe^{II}(CO)]$ was prepared same manner in THF as solvent and similar results are observed for $[(P^{Im})Fe^{II}(CO)]$ with a λ_{max} (ε/mM^{-1} cm^{-1}): 421 (279.5), 538 (25.1) (Fig. S4b), the same value for $\nu_{(C-O)}$ = 1985 cm^{-1} (Table 2) (Fig. S5c) and a diamagnetic ^1H NMR showing the pyrrole hydrogens at δ 8.5 ppm and imidazole hydrogens shifted upfield to δ 3 ~5 ppm (Fig. S6b), again evidence for a low-spin Fe^{II} ($S = 0$, d^6) six coordinate $[(P^{Im})Fe^{II}(CO)]$ complex. Somewhat surprisingly, while one might expect that a stronger axial trans donor (e.g., imidazolyl > pyridyl > THF) would lead to a measurably reduced the C–O stretching frequency, the data here shows that does not seem to be the case. However, this finding has precedent; a lack of correlation of $\nu_{(C-O)}$ with base strength is observed for a number of other cases [28,29,43].

3. Conclusions

In summary, we have described here the synthesis of hemes with covalently tethered axial base ligands for iron, either a pyridyl or imidazolyl group. Reduced iron(II) porphyrinates have been synthesized and compared to a closely related iron(II) complex not possessing the tailed base, $[(F_8)Fe^{II}]$. Comparison of the solution properties of the three iron(II) complexes and their O_2 or CO adducts has been carried out using multinuclear NMR, UV–Vis and IR spectroscopies. The spin state of iron in the complexes $[(F_8)Fe^{II}]$, $[(P^{Py})Fe^{II}]$ and $[(P^{Im})Fe^{II}]$ depends on solvent employed. We have generated and characterized two new low-spin O_2-adducts, the six-coordinate heme–Fe–superoxo complexes $[(P^{Py})Fe^{III}(O_2^{\cdot-})]$ and $[(P^{Im})Fe^{III}(O_2^{\cdot-})]$, and two new low-spin six coordinate heme–Fe–CO complexes $[(P^{Py})Fe^{II}(CO)]$ and $[(P^{Im})Fe^{II}(CO)]$, with tailed base as the axial ligand. The reversibility of O_2-binding to reduced complexes has been established by UV–Vis spectroscopy, following either oxygenation by O_2-bubbling or deoxygenation via purging solutions of $[(P^{Py})Fe^{III}(O_2^{\cdot-})]$ or $[(P^{Im})Fe^{III}(O_2^{\cdot-})]$ with argon gas.

The longer term goal of our research, the main reason for synthesizing such complexes with P^{Py} and P^{Im}, is to utilize derived iron(II) or Fe(III)–superoxo compounds to generate new heme–Fe^{III}–((hydro)peroxo)–Cu^{II} species [20,52,53], of possible relevance to the active site chemistry occurring in cytochrome *c* oxidase [20,54]. We have already shown that addition of a strong 'base' (e.g., dicyclohexylimidazole) to a heme–peroxo–copper assembly can have a large influence with respect to subsequent O–O cleavage when protons and/or electrons are added (where a phenol was used as a hydrogen atom source) [19,20]. The new heme–Fe^{II}–CO species will be employed in the initiation of CO flash photolysis investigations using laser pulses to photoeject CO and observe either CO (as an O_2-surrogate) or O_2 (flash-and-trap) rebinding

[2] We have recently obtained resonance Raman data for $[(P^{Im})Fe^{III}(O_2^{\cdot-})]$, and the O–O and Fe–O stretching frequencies are essentially identical to those for $[(THF)(F_8)Fe^{III}(O_2^{\cdot-})]$ and for heme proteins, K.D. Karlin and co-workers, unpublished observations.

[32,33,35,36], to probe how the kinetics and thermodynamics of binding to heme or copper is affected by the ligand environment. Such investigations should provide fundamental information relevant to other synthetic chemical systems (and thus potentially catalytic processes) as well as to biological systems using iron and/or Cu in the utilization of molecular oxygen.

4. Experimental

4.1. Materials

All reagents and solvents purchased and used were of commercially available quality except as noted. All the air sensitive compounds and reactions were handled under an Ar atmosphere by applying Schlenk techniques or prepared in an MBraun glovebox filled with nitrogen (O_2, H_2O < 1 ppm). Dichloromethane (CH_2Cl_2) was purified and dried over an activated alumina column under a nitrogen atmosphere. Acetone was distilled over Drierite (97% $CaSO_4$, 3% $CoCl_2$) under Ar. Tetrahydrofuran (THF) was distilled over sodium/benzophenone under Ar. All solvents were degassed with argon bubbling for 30 min or by three freeze/pump/thaw cycles before transferring into the glovebox. Dioxygen gas (4.4 Grade) was purchased from Air Gas East and dried by passage through a column of $CaSO_4$. Carbon monoxide gas (2.3 Grade) was used as received from Air Gas East and dried by passage through an R&D separation oxygen/moisture trap model OT3-4.

4.2. Methods

All the UV–Vis measurements were carried out by using a Hewlett Packard 8453 diode array spectrophotometer with a quartz cuvette (path length = 10 mm). The spectrometer was equipped with a HP Chemstation software and Unisoku thermostated cell holder for low temperature experiments. In a typical reaction, the quartz cuvette was usually filled with 2.7 mL (1 μM) starting solution of heme–Fe^{II} complex prepared and sealed in the glovebox and then taken to the benchtop where it was cooled in the thermostated cell holder. Then, O_2 or CO was bubbled through cold solution via a 10-inch needle hooked to the gas tank.

All NMR spectra were recorded in 7 inch, 5 mm o.d. NMR tubes. ^1H NMR was performed on Bruker 300 or 400 MHz NMR instrument while ^2H NMR were carried out on a Varian 500 MHz NMR instrument equipped with a tunable deuterium probe to enhance deuterium detection. The $^{1,2}H$ chemical shifts are calibrated to natural abundance deuterium or proton solvent peaks. In a typical reaction, the NMR tube was loaded with 0.5 mL (10 mM) solution of heme–Fe^{II} prepared and sealed in glovebox then cooled in a cold bath. Then O_2 was bubbled very slowly through cold solution via a 10-inch needle hooked to a syringe filled with O_2. CO was bubbled through room temperature solution via a 10-inch needle hooked to the carbon monoxide tank.

Electrospray ionization mass spectrometry (ESI-MS) spectra were acquired using a Finnigan LCQ Duo ion-trap mass spectrometer equipped with an electrospray ionization source (Thermo Finnigan, San Jose, CA). The heated capillary temperature was 250 °C and the spray voltage was 5 kV. Spectra were recorded continuously after injection.

Infrared spectroscopy (IR) spectra were collected using a Thermo Scientific Nicolet Nexus 670 FT-IR spectrophotometer. A solution of heme–Fe^{II} was prepared the same way as for NMR spectroscopy and then injected into a 25 μm path length solution flow cell (using two CaF_2 windows: one with a sensitized thin film and the other without a thin film) via a 1 mL syringe to take an IR spectrum as background. Then, CO was bubbled into the stock solution in the NMR tube and in a similar manner loaded into the solution IR cell to obtain the carbonyl C–O stretching frequencies. The measurements were taken in transmission mode and averaged by 32 scans with 2 cm^{-1} resolutions.

4.3. Synthesis

The reduced heme–Fe^{II} complexes [$(F_8)Fe^{II}$] and [$(d_8\text{-}F_8)Fe^{II}$] were prepared following previously reported procedures [14,15,41,55]. The free porphyrin ligands P^{Py} and P^{Im} were synthesized using published procedures [37] but with modifications presented here. The precursor porphyrins $F_6(NO_2)$ (=5,10,15-tris-(2,6-difluoro-phenyl)-20-(2-nitro-phenyl)-porphyrine) [56], $F_6(NO_2)$-d_8 (=5,10,15-Tris-(2,6-difluoro-phenyl)-20-(2-nitro-phenyl)-porphyrine-d_8) [57] and $F_6(NH_2)$ (=2-[10,15,20-tris-(2,6-difluoro-phenyl)-porphyrin-5-yl]-phenylamine) [56] were synthesized using the procedures in the references cited. $F_6(NH_2)$-d_8 (=2-[10,15,20-Tris-(2,6-difluoro-phenyl)-porphyrin-5-yl]-phenylamine-d_8) were prepared as reported for $F_6(NH_2)$ [56] but employing $F_6(NO_2)$-d_8 in place of $F_6(NO_2)$.

P^{Py}. A mixture of 3-(3′-pyridyl) propionic acid (1.56 g, 10.3 mmol) and 100 mL $CHCl_3$ were placed in a 500 mL round bottom flask and heated to 60 °C. Thionyl chloride ($SOCl_2$) (10 mL) was added and the solution stirred for 4 h at 60 °C. The resulting mixture was evacuated to remove excess $SOCl_2$ and solvent. The solid residue was re-dissolved in 20 mL CH_2Cl_2 at room temperature. To this, the $F_6(NH_2)$ (1.90 g, 2.58 mmol) was dissolved in 25 mL CH_2Cl_2 and the solution was added dropwise, followed by the addition of 1.5 mL pyridine. The resulting mixture was stirred for 30 min. The excess pyridine and solvent were removed under vacuum. The resulting solid mixture was re-dissolved in 250 mL CH_2Cl_2 and washed with deionized H_2O several times. The organic layer was saved and dried over anhydrous $MgSO_4$ followed by filtration of $MgSO_4$ and solvent removal using rotary evaporation. The product obtained was purified by column chromatography (silica, ethyl acetate/hexane = 4:1). Yield: 1.56 g, 70%. ^1H NMR (400 MHz, $CDCl_3$): δ 8.99–8.73 (m, 8H, pyrrole-H), 8.64 (m, 1H, amimophenyl), 8.06 (m, 1H, aminophenyl), 7.93 (m, 1H, pyridyl), 7.72(m, 5H, diflurophenyl (3H) and aminophenyl (2H)), 7.52 (m, 1H, pyridyl), 7.38 (m, 6H, diflurophenyl), 6.68 (s, 1H, –NH–C=O), 6.53 (m, 1H, pyridyl), 6.42 (m, 1H, pyridyl), 2.3–2.1 (m, 4H, -CH_2-CH_2-Pyridyl), −2.78 (s, 2H, NH pyrrole) (Fig. S6). ESI-MS (*m/z*): 871 $(M+H^+)^+$.

P^{Py}-d_8. The pyrrole deuterated porphyrin ligand P^{Py}-d_8 was prepared using a procedure identical to that described above for P^{Py}, but employing the pyrrole deuterated porphyrin $F_6(NH_2)$-d_8 instead of $F_6(NH_2)$. ^2H NMR (400 MHz, $CHCl_3$): δ 8.99–8.73 (m, 8H, pyrrole-D). ESI-MS (*m/z*): 879 $(M+H^+)^+$.

$(P^{Py})Fe^{III}Cl$. The ligand P^{Py} (1.44 g, 1.5 mmol) was dissolved in 20 mL THF under an argon atmosphere. Iron(II) chloride tetrahydrate (7 g, 55.2 mmol) was added and the solution was heated to reflux at 60 °C under argon for 3 h. After cooling to room temperature, the solution was exposed to air and stirred for 3 h. The solvent was removed by rotary evaporation and the residue obtained was re-dissolved in 100 mL CH_2Cl_2 followed by filtering the insoluble solid present. The solution was stirred with HCl (1 M, 100 mL) for 3 h and then neutralized using solid $NaHCO_3$. The organic layer was washed with 100 mL saturated $NaHCO_3$ then NaCl water solution and dried over anhydrous $MgSO_4$. The desired product was purified by column chromatography (silica, CH_2Cl_2/MeOH = 98:2). Yield: 1.08 g, 68%. UV–Vis [nm]: CH_2Cl_2, 334, 413, 574; THF, 335, 415, 565. ^1H NMR (400 MHz, THF-d_8): δ 80 (s, br, pyrrole-H). ESI-MS (*m/z*): 924 $(M-Cl^-)^+$.

$(P^{Py})Fe^{II}$. The degased solution of $P^{Py}Fe^{III}Cl$ (500 mg, 0.5 mmol) in 40 mL CH_2Cl_2 was added to the degassed 50 mL saturated $Na_2S_2O_{4\,(aq)}$ solution under an argon atmosphere. The two solutions were mixed using argon bubbling for 30 min in an additional funnel. The reaction mixture was allowed to sit for 20 min until the two layers

separated. The organic layer was separated and passed through anhydrous Na_2SO_4 powder loaded in a filter tube (one end connecting to the additional funnel and the other end connecting to a Schlenk flask) under an argon atmosphere. Then the solvent was removed and dried in vacuo for 3 h. The resulting solid was kept in glove box. Yield: 488.6 mg, 92%. UV–Vis [nm] in THF: 417, 524, 553. ^{1}H NMR (400 MHz, THF-d_8): δ 50, 58 (s, br, pyrrole-H) (Fig. S1). ESI-MS (m/z): 924 $(M-e^-)^+$.

$(P^{Py})Fe^{II}$-d_8. The pyrrole deuterated heme–Fe^{II} $(P^{Py})Fe^{II}$-d_8 was prepared using identical procedure to that described above for $(P^{Py})Fe^{II}$, but employing pyrrole deuterated porphyrin P^{Py}-d_8 instead of P^{Py}. ^{2}H NMR (400 MHz, THF): δ 50, 58 (s, br, pyrrole-D). ESI-MS (m/z): 932 $(M-e^-)^+$.

$F_6(NHCOBzCH_2Cl)$. The porphyrin $F_6(NH_2)$ (1.3 g, 1.77 mmol, 1 equiv) was dissolved in 100 mL THF under an argon atmosphere. Triethylamine (1.04 mL, 4 equiv) was added and the solution was cooled to 0 °C followed by the addition of 3-(chloromethyl)-benzoylchloride (0.4 mL, 1.5 equiv) dropwise. The solution was stirred for 3 h at 0 °C. Then excess triethylamine and solvent were removed under a vacuum. The resulting product was purified by column chromatography (silica, CH_2Cl_2). Yield: 1.2 g, 77%. ^{1}H NMR (400 MHz, CDCl3): δ 8.76 (m, 8H, pyrrole-H), 8.15 (m, 1H, amimophenyl), 7.88 (m, 1H, aminophenyl), 7.73 (m, 4H, *para* diflurophenyl (3H) and aminophenyl (1H)), 7.58(m, 1H, aminophenyl), 7.34 (m, 6H, *ortho* diflurophenyl), 6.78 (m, 2H, benzyl–C═O), 6.72 (s, 1H, –NH–C═O), 6.34 (m, 1H, benzyl–C═O), 6.14 (m, 1H, benzyl–C═O), 3.68 (s, 1H, benzyl-CH_2-Cl), −2.72 (s, 2H, NH pyrrole). ESI-MS (m/z): 891 $(M+H^+)^+$.

P^{Im}. The porphyrin $F_6(NHCOBzCH_2Cl)$ (1.1 g, 1.24 mmol, 1 equiv) was dissolved in a solvent mixture of 150 mL dry toluene and 150 mL dry ethanol under an argon atmosphere. Imidazole (25 g, 300 equiv) and NaI (741 mg, 4 equiv) were added and the solution was heated to 62 °C and stirred in the dark and under an argon atmosphere for 12 h. The solution was then cooled to RT and solvent was removed by rotary evaporation. The solid residue obtained was re-dissolved in 50 mL CH_2Cl_2 and was twice washed with 400 mL deionized H_2O. The organic layer was saved and dried over anhydrous $MgSO_4$ and this was followed by filtration of the $MgSO_4$ and solvent removal using rotary evaporation. The product obtained was purified by column chromatography in the dark (silica, 0.1% triethylamine, 1% MeOH/CH_2Cl_2). Yield: 800 mg, 70%. ^{1}H NMR (400 MHz, $CDCl_3$): δ 8.86–8.78 (m, 9H, pyrrole (8H) and aminophenyl (1H)), 8.11 (dd, 1H, benzyl), 7.84–7.71 (m, 4H, *para* diflurophenyl (3H) and aminophenyl (1H)), 7.52 (m, 1H, aminophenyl), 7.46–7.25 (m, 8H, meta diflurophenyl (6H) and benzyl (2H)), 6.78 (s, 1H, –NH–C═O), 6.35–6.24 (m, 4H, benzyl (1H), aminophenyl (1H) and imidazolyl (2H)), 6.08 (s, 1H, imidazolyl), 3.73 (s, 2H, –CH_2–benzyl), −2.79 (s, 2H, NH pyrrole) (Fig. S6). ESI-MS (m/z): 923 $(M+H^+)^+$.

P^{Im}-d_8. The pyrrole deuterated porphyrin ligand P^{Im}-d_8 was prepared using identical procedure to that described above for P^{Im}, but employing pyrrole deuterated porphyrin $F_6(NH_2)$-d_8 instead of $F_6(NH_2)$. ^{2}H NMR (400 MHz, $CHCl_3$): δ 8.86–8.78 (m, 8H, pyrrole-D). ESI-MS (m/z): 931 $(M+H^+)^+$.

$(P^{Im})Fe^{III}(OH)$. The ligand P^{Im} (700 mg, 0.76 mmol) was dissolved in 20 mL THF under an argon atmosphere. Iron(II) chloride tetrahydrate (7 g, 55.2 mmol) was added and the solution was heated to reflux at 60 °C under an argon atmosphere for 3 h. After cooling to RT, the solution was exposed to air and stirred for 3 h. The solvent was removed by rotary evaporation and the residue was re-dissolved in 100 mL CH_2Cl_2 and this was followed by filtering the insoluble solid present. The solution was stirred with NaOH (3 M, 100 mL) for 3 h. The organic layer was washed with NaOH solution (2 M, 100 mL) and water three times and then dried over anhydrous $MgSO_4$. The desired product was purified by column chromatography (silica, CH_2Cl_2/MeOH = 98:2). Yield: 572 mg, 76%. UV–Vis [nm] in THF, 414, 541. ^{1}H NMR (400 MHz, THF-d_8): δ 80 (s, br, pyrrole-H). ESI-MS (m/z): 975 $(M-OH^-)^+$.

$(P^{Im})Fe^{II}$. A degassed solution of $P^{Im}Fe^{III}(OH)$ (500 mg, 0.5 mmol) dissolved in 40 mL CH_2Cl_2 was added to the degassed 50 mL saturated $Na_2S_2O_4$ and $Na_2CO_{3\,(aq)}$ solution under an argon atmosphere. The two solutions were mixed by argon bubbling for 30 min in an additional funnel. The reaction mixture was allowed to sit for 20 min until the two layers separated. The organic layer was separated and passed through anhydrous Na_2SO_4 powder loaded in a filter connecting to the additional funnel (one end connecting to the additional funnel and the other end connecting to a Schlenk flask) under an argon atmosphere. Then the solvent was removed and dried by vacuum for 3 h. The resulting solid was kept in glove box. Yield: 442 mg, 90%. UV–Vis [nm] in THF: 417, 524, 553. ^{1}H NMR (400 MHz, acetone-d_6): δ 41, 60 (s, br, pyrrole-H) (Fig. S2). ESI-MS (m/z): 975 $(M-e^-)^+$.

$(P^{Im})Fe^{II}$-d_8. A procedure identical to that given above for $(P^{Im})Fe^{II}$ was used but employing pyrrole deuterated P^{Im}-d_8 instead of P^{Im}. ^{2}H NMR (400 MHz, THF): δ 8.4, 10.9, 12.6 (s, pyrrole-D) (Fig. S2). ESI-MS (m/z): 983 $(M-e^-)^+$.

Acknowledgement

This work was supported by the National Institutes of Health (R01 GM 060353 to K.D.K).

Appendix A. Supplementary data

Supplementary data associated with this article can be found, in the online version, at http://dx.doi.org/10.1016/j.poly.2012.11.011.

References

[1] I. Bertini, H.B. Gray, E.I. Stiefel, J.S. Valentine (Eds.), Biological Inorganic Chemistry – Structure and Reactivity, University Science Books, Sausalito, CA, 2007.
[2] T.G. Spiro (Ed.), Metal Ion Activation of Dioxygen: Metal Ions in Biology, vol. 2, Wiley-Interscience, New York, 1980.
[3] S. Ferguson-Miller, G.T. Babcock, Chem. Rev. 96 (1996) 2889.
[4] T. Tsukihara, H. Aoyama, E. Yamashita, T. Tomizaki, H. Yamaguchi, K. Shinzawa-Itoh, R. Nakashima, R. Yaono, S. Yoshikawa, Science 269 (1995) 1069.
[5] S. Iwata, C. Ostermeier, B. Ludwig, H. Michel, Nature 376 (1995) 660.
[6] J.P. Collman, R. Boulatov, C.J. Sunderland, Porphyrin Handbook 11 (2003) 1.
[7] E. Kim, E.E. Chufán, K. Kamaraj, K.D. Karlin, Chem. Rev. 104 (2004) 1077.
[8] C. Varotsis, Y. Zhang, E.H. Appelman, G.T. Babcock, Proc. Natl. Acad. Sci. U.S.A. 90 (1993) 237.
[9] M. Momenteau, C.A. Reed, Chem. Rev. 94 (1994) 659.
[10] J.S. Olson, G.N. Phillips Jr., J. Biol. Inorg. Chem. 2 (1997) 544.
[11] J.P. Collman, C.J. Sunderland, K.E. Berg, M.A. Vance, E.I. Solomon, J. Am. Chem. Soc. 125 (2003) 6648.
[12] C. Ruzie, P. Even, D. Ricard, T. Roisnel, B. Boitrel, Inorg. Chem. 45 (2006) 1338.
[13] R.A. Ghiladi, K.D. Karlin, Inorg. Chem. 41 (2002) 2400.
[14] R.A. Ghiladi, R.M. Kretzer, I. Guzei, A.L. Rheingold, Y.-M. Neuhold, K.R. Hatwell, A.D. Zuberbühler, K.D. Karlin, Inorg. Chem. 40 (2001) 5754.
[15] K.D. Karlin, A. Nanthakumar, S. Fox, N.N. Murthy, N. Ravi, B.H. Huynh, R.D. Orosz, E.P. Day, J. Am. Chem. Soc. 116 (1994) 4753.
[16] R.A. Ghiladi, T.D. Ju, D.-H. Lee, P. Moënne-Loccoz, S. Kaderli, Y.-M. Neuhold, A.D. Zuberbühler, A.S. Woods, R.J. Cotter, K.D. Karlin, J. Am. Chem. Soc. 121 (1999) 9885.
[17] R.A. Ghiladi, K.R. Hatwell, K.D. Karlin, J. Am. Chem. Soc. 123 (2001) 6183.
[18] E.E. Chufán, S.C. Puiu, K.D. Karlin, Acc. Chem. Res. 40 (2007) 563.
[19] M.T. Kieber-Emmons, M.F. Qayyum, Y. Li, Z. Halime, K.O. Hodgson, B. Hedman, K.D. Karlin, E.I. Solomon, Angew. Chem., Int. Ed. 51 (2012) 168.
[20] Z. Halime, M.T. Kieber-Emmons, M.F. Qayyum, B. Mondal, T. Gandhi, S.C. Puiu, E.E. Chufán, A.A.N. Sarjeant, K.O. Hodgson, B. Hedman, E.I. Solomon, K.D. Karlin, Inorg. Chem. 49 (2010) 3629.
[21] J.P. Collman, J.I. Brauman, T.R. Halbert, K.S. Suslick, Proc. Natl. Acad. Sci. U.S.A. 73 (1976) 3333.
[22] O. Einarsdottir, R.B. Dyer, D.D. Lemon, P.M. Killough, S.M. Hubig, S.J. Atherton, J.J. Lopez-Garriga, G. Palmer, W.H. Woodruff, Biochemistry 32 (1993) 12013.
[23] T.G. Spiro, I.H. Wasbotten, J. Inorg. Biochem. 99 (2005) 34.
[24] T.G. Spiro, P.M. Kozlowski, Acc. Chem. Res. 34 (2001) 137.
[25] R.W. Larsen, J. Miksovska, Coord. Chem. Rev. 251 (2007) 1101.
[26] S. Aono, Dalton Trans. (2008) 3137.
[27] T.L. Poulos, Nat. Prod. Rep. 24 (2007) 504.

[28] N.J. Silvernail, B.C. Noll, C.E. Schulz, W.R. Scheidt, Inorg. Chem. 45 (2006) 7050.
[29] N.J. Silvernail, A. Roth, C.E. Schulz, B.C. Noll, W.R. Scheidt, J. Am. Chem. Soc. 127 (2005) 14422.
[30] Q.H. Gibson, C. Greenwood, Biochem. J. 86 (1963) 541.
[31] C. Greenwood, Q.H. Gibson, J. Biol. Chem. 242 (1967) 1782.
[32] H.C. Fry, D.V. Scaltrito, K.D. Karlin, G.J. Meyer, J. Am Chem. Soc. 125 (2003) (1871) 11866.
[33] H.C. Fry, A.D. Cohen, J.P. Toscano, G.J. Meyer, K.D. Karlin, J. Am. Chem. Soc. 127 (2005) 6225.
[34] R.M. Kretzer, R.A. Ghiladi, E.L. Lebeau, H.-C. Liang, K.D. Karlin, Inorg. Chem. 42 (2003) 3016.
[35] H.R. Lucas, G.J. Meyer, K.D. Karlin, J. Am. Chem. Soc. 131 (2009) 13924.
[36] F. Melin, A. Trivella, M. Lo, J. Inorg. Biochem. 108 (2012) 196.
[37] T.C. Berto, V.K.K. Praneeth, L.E. Goodrich, N. Lehnert, J. Am. Chem. Soc. 131 (2009) 17116.
[38] H. Goff, G.N. La Mar, J. Am. Chem. Soc. 99 (1977) 6599.
[39] A. Shirazi, H.M. Goff, J. Am. Chem. Soc. 104 (1982) 6318.
[40] F.A. Walker, U. Simonis, Proton NMR Spectroscopy of Model Hemes, in: L.J. Berliner, J. Reuben (Eds.), Biological Magnetic Resonance, Plenum Press, New York, 1993, pp. 133–274 (vol. 12/NMR of Paramagnetic Molecules).
[41] M.-A. Kopf, Y.-M. Neuhold, A.D. Zuberbühler, K.D. Karlin, Inorg. Chem. 38 (1999) 3093.
[42] F.A. Walker, Proton NMR and EPR spectroscopy of paramagnetic metalloporphyrins, in: K.M. Kadish, K.M. Smith, R. Guilard (Eds.), The Porphyrin Handbook, Academic Press, San Diego, 2000, pp. 81–184 (vol. 5/NMR and EPR).
[43] D.W. Thompson, R.M. Kretzer, E.L. Lebeau, D.V. Scaltrito, R.A. Ghiladi, K.-C. Lam, A.L. Rheingold, K.D. Karlin, G.J. Meyer, Inorg. Chem. 42 (2003) 5211.
[44] E. Kim, M.E. Helton, I.M. Wasser, K.D. Karlin, S. Lu, Proc. Natl. Acad. Sci. U.S.A. 100 (2003) 3623.
[45] I.M. Wasser, H.W. Huang, P. Moenne-Loccoz, K.D. Karlin, J. Am. Chem. Soc. 127 (2005) 3310.
[46] A.L. Balch, Y.W. Chan, R.J. Cheng, G.N. La Mar, L. Latos-Grazynski, M.W. Renner, J. Am. Chem. Soc. 106 (1984) 7779.
[47] A.L. Balch, Inorg. Chim. Acta 198–200 (1992) 297.
[48] H. Brunner, Naturwissenschaften 61 (1974) 129.
[49] L.L. Duff, E.H. Appelman, D.F. Shriver, I.M. Klotz, Biochem. Biophys. Res. Commun. 90 (1979) 1098.
[50] K. Nakamoto, Infrared and Raman Spectra of Inorganic and Coordination Compounds, vol. Part B, fifth ed., Wiley Interscience, New York, 1997, p. 330
[51] K. Nakamoto, Infrared and Raman Spectra of Inorganic and Coordination Compounds, vol. Part B, fifth ed., Wiley Interscience, New York, 1997, p. 161.
[52] E.E. Chufan, B. Mondal, T. Gandhi, E. Kim, N.D. Rubie, P. Moenne-Loccoz, K.D. Karlin, Inorg. Chem. 46 (2007) 6382.
[53] Z. Halime, H. Kotani, Y. Li, S. Fukuzumi, K.D. Karlin, Proc. Natl. Acad. Sci. U.S.A. 108 (2011) 13990.
[54] Z. Halime, K.D. Karlin, Cytochrome c oxidase and models, in: S. Itoh, K.D. Karlin (Eds.), Copper–Oxygen Chemistry, vol. 4, John Wiley & Sons, Inc., Hoboken, 2011, pp. 283–319.
[55] A. Nanthakumar, Inorg. Chem. 30 (1991) 4460.
[56] E. Kim, J. Shearer, S. Lu, P. Moënne-Loccoz, M.E. Helton, S. Kaderli, A.D. Zuberbühler, K.D. Karlin, J. Am. Chem. Soc. 126 (2004) 12716.
[57] E. Kim, M.E. Helton, S. Lu, P. Moënne-Loccoz, C.D. Incarvito, A.L. Rheingold, S. Kaderli, A.D. Zuberbühler, K.D. Karlin, Inorg. Chem. 44 (2005) 7014.
[58] J.-G. Liu, Y. Shimizu, T. Ohta, Y. Naruta, J. Am. Chem. Soc. 132 (2010) 3672.
[59] J.-G. Liu, T. Ohta, S. Yamaguchi, T. Ogura, S. Sakamoto, Y. Maeda, Y. Naruta, Angew. Chem., Int. Ed. 48 (2009) 9262.